

MULTIFUNCTIONAL PAMAM-SURFACE NANOSTRUCTURED PARTICLES ORGANIZED IN MULTIMERIC CLUSTERS. POTENTIAL SMART DELIVERY VEHICLES OF BIOACTIVE SPECIES THROUGH A HIGH SELECTIVE AMINE-THIOL BIOCONJUGATION STRATEGY

I. C. STANCU^{*}, A. LUNGU, E. RUSEN, A. MOCANU, P. Z. IORDACHE^b, D. M. DRAGUSIN, C. COTRUT^a, E. VASILE^c, H. IOVU

Department of Polymer Chemistry and Engineering, Faculty of Applied Chemistry and

Materials Science, Polytechnics University of Bucharest, Calea Victoriei 149, sector 1, Bucharest, 010072, Romania

^aUniversity POLITEHNICA of Bucharest, Faculty of Materials Science and Engineering, 313 Splaiul Independentei, 060042, sector 6, Bucharest, Romania

^bCBRN Defense and Ecology Scientific Research Center, 225 Șos. Olteniței, 041309 Bucharest, Romania

^cMETAV Research & Development, 31 C.A. Rosetti, sector 2, Bucharest, Romania

The present work is devoted to the investigation of the polyamidoamine (PAMAM) dendrimer binding on the surface of polymer particles. Two generations of amino-terminal PAMAM macromolecules were chemically immobilized on the outer epoxy-shell of the polymer leading to nanostructured surface further available for cluster-like binding of a wide range of chemical species. The study proved that nanostructuring was successful and even enhanced by higher generation dendrimer. Multimeric clusters of functionalized particles were formed through physical interactions. Furthermore, the study was continued with the activation of the reactive amino-shell with a heterobifunctional reagent allowing the high-specific immobilization of thiol-containing species. A model thiol-ended peptide, glutathione, has been used to prove the efficiency of the cluster-type delivery system synthesized here. These materials open a generous route of creating solid surface nanostructured undermicronic particles decorated with chemically linked bioactive (and not only) molecules, to be further included in more complex scaffolds.

(Received October 16, 2010; accepted November 26, 2010)

Keywords: Clusters; Dendrimers; Nanorough surface; Glutathione

1. Introduction

Two of the top challenges in the field of hard tissue (HT) engineering remain the development of bio-inspired materials and the increased bioactivity of the biomaterials.

Bone and teeth present structural units organized on macro-, micro- and nano- levels. The design of a biomaterial should address all these organization levels. Thus, macroscopic (dimensional stability, hydrophilicity, mechanical strength, etc.) and microscopic (porosity, phase segregation, local electrical charge, etc.) characteristics may be ensured through a convenient selection of the scaffold material. In this respect, starting from the apatite-collagenic nature of HT, different ceramics and polymers have been tested and used for a wide range of biomedical application in HTE. However, providing a macro- and micro-organized scaffold with nano-features remains still very important when aiming HT regeneration. The crystallite average size in

^{*}Corresponding author: izabela.cristina.stancu@gmail.com

nanomaterials is under 100 nm. The mechanism governing the superior performances of HT in contact with nanomaterials is due to the fact that HT cells are naturally accustomed with a nanometric scaled physiological environment, represented by the natural constituents of healthy bone and teeth (HA crystals, fibrillar collagen etc.). The years 2000s have turned the attention on the effect of nanomaterials in bone regeneration. Works converge to the conclusion that the response of host organisms to the presence of nanomaterials, including the cellular and proteic levels, is different and certainly superior when compared with conventional materials used until present [1-10]. This work is devoted to the engineering of smart materials with cluster-like architecture and functionality, very efficient for specific delivery of different bioactive species. The first part of the study reports the development of materials consisting in undermicronic size polymer particles surface-nanostructured with polyamidoamine (PAMAM) dendrimers. PAMAM present nano- dimensions and their presence onto the surface of a material leads to structural features within this dimensional range. Their use as coating of different surfaces providing nanoroughness, increased chemical reactivity and thus enhanced bioactivity has been explored recently [11-14]. The influence of the dendrimer generation on the surface morphology of the polymer beads is investigated.

The study began with the PAMAM binding onto the polymer beads, followed by the development of two types of amino-functional clusters.

In the second part, the amino- reactive shell of the nanostructured polymer particles is used to explore their potential to be specifically biofunctionalized. Due to the high reactivity of amino-groups the functionality of the target molecules to be conjugated onto these smart delivery vehicles may be impressively wide, ranging from carboxyl, hydroxyl, epoxy, carbonyl, amines, and nevertheless thiols. Different chemical protocols are well-known in the literature for this purpose [15]. This work basically refers to a simple but highly selective approach: the amino-groups are activated using a hetero-bifunctional reagent and then the specific bioconjugation with a model thiol-containing peptide is exemplified. 3-(2-Pyridyldithio)propionic acid N-hydroxysuccinimide ester (SPDP) was selected as crosslinking agent due to its specificity against primary amines and thiol groups. The chemical strategy is based on a two steps procedure: a first coupling reaction with primary amine groups from the outer shell of the immobilized PAMAM followed by a second coupling needed to bind the bioactive species; the latter occurs by thiol disulfide exchange between 2-pyridyldithio sequence and the sulfhydryl group of the reactive peptide (here glutathione). This chemical approach provides high selectivity with respect to the interacting species (activated amino- groups and free thiols).

This work addresses the field of the smart biofunctionalization through a wide range of possibilities of obtaining surface-nanoengineered and multibiofunctional-materials and through the availability of the latter for physical incorporation in other biomaterials.

2. Experimental

Materials

Styrene – St (from Merck) was purified through distillation under vacuum. 2-hydroxyethyl methacrylate – HEMA and (2,3-epoxypropyl)-methacrylate – GMA were purchased from Sigma-Aldrich and were passed through separation columns filled with Al_2O_3 to remove inhibitors. Potassium persulphate (KPS) (Merck) was recrystallized from a mixture ethanol/water and then vacuum dried. Polyamidoamine dendrimers, generation 2 (PAMAM2) and generation 4 (PAMAM4) were supplied from Sigma-Aldrich as solutions in methanol (20% and 10%, respectively) and used as received.

SPDP (>95%), L-glutathione reduced – GSH, pyridine-2-thione - Py-2-thione (99%) and 1,2-phthalic dicarboxyaldehyde – OPA (98%+) and n-butyl amine (n-Bu) were supplied from Sigma-Aldrich and used as received. Analytical grade 2-mercaptoethanol - ME was supplied from Merck, ethanol absolute SPECTRANAL® from Riedel-de Haën and tetrahydrofurane CHROMASOLV® - THF from Sigma-Aldrich. All the salts necessary to prepare phosphate buffer

(PBS) pH 7.4 and the buffer pH 10 needed for OPA method were supplied by Sigma-Aldrich. MilliQ water was used for the reactions and distilled water for the dialysis.

Synthesis of the polymer latex. The particles used as a substrate in this study were obtained through a two step polymerization procedure consisting in an initial soap-free polymerization described in a different work [16], followed by a convenient seeded polymerization leading to an amino-reactive epoxy shell.

Soap-free emulsion polymerization. 6.5 ml St and 2 ml HEMA were added in 100 ml distilled water, using 0.0625g of KPS. The reaction mixture was nitrogen purged and then maintained for 48 h at 75°C under continuous stirring. The final St-HEMA latex was purified through dialysis against distilled water for 7 days, using cellulose dialysis membranes (molecular weight cutoff: 12.000-14.000).

Seeded emulsion polymerization. 2 ml GMA and 0.08g KPS were added to 70 ml of preformed St-HEMA latex, followed by nitrogen bubbling and then by stirring at 75°C, for 24 h. The modified latex was dialyzed in distilled water for 7 days. The obtained particles are further denoted as P-GMA.

PAMAM-grafting of the polymer latex. PAMAM methanolic solution has been directly added to 12 ml of P-GMA latex containing polymer particles (0.38g), under vigorous stirring. The concentration of the dendrimer in the final reaction mixture was 0.1 mM. The reaction was allowed to occur for 24 hours, at room temperature. Then, the mixtures were dialyzed against distilled water, for 24 hours. The resulting dialysis water was kept for dendrimer detection through a UV-VIS spectrometric method as further detailed. The resulted particles were named P-PAMAM2 and P-PAMAM4 according to the generation of the dendrimer.

SPDP-crosslinking. Free NH₂-groups from the P-PAMAM2 and P-PAMAM4 were further activated with SPDP for specific reactions with thiol-containing species. SPDP was previously dissolved in THF (to reach a concentration of 6,2 mg/ml) as recommended in [15], and then it has been dropwise added to the reaction mixture to directly react with with free -NH₂. 1:10 and 1:100 molar ratios were used between SPDP and theoretically free -NH₂ in P-PAMAM2 and P-PAMAM4, respectively. The chemical interaction occurs between -NH₂ and the amino-reactive succinimidyl group of the SPDP hetero-bifunctional reagent, at room temperature, under inert atmosphere and under stirring, for 24 hours. The reaction products were washed with methanol for 30 minutes and then dialysed against distilled water, for 24 hours at room temperature, and then dried. For simplicity, the obtained materials were named PAMAM2-SPDP and PAMAM4-SPDP, according to the generation of the dendrimer immobilized onto the polymer surface. These are bioconjugation intermediates.

Peptide coupling. PAMAM2-GSH and PAMAM4-GSH bioconjugates were prepared through the direct reaction between the PAMAM2(4)-SPDP intermediates and the model peptide GSH. Stoichiometric amount of GSH has been used (corresponding to the ration needed to modify all SPDP residues from the PAMAM2(4)-SPDP). As example, the preparation of PAMAM2-GSH is presented. 50 mg of dried PAMAM2-SPDP intermediate manually grinded in a mortar and redispersed by ultrasounds in 10 mL PBS pH 7.4, under argon, at room temperature, and under stirring. The corresponding amount of GSH was dissolved in 3 mL PBS pH 7.4, under argon, at room temperature and under stirring. The peptide solution was dropwise added to the PAMAM2-SPDP solution. After the reaction, the particles were dialysed against MilliQ water to remove unreacted GSH and the Py-2-thione formed during the reaction. The dialysis was carried out for 24 hours, at room temperature. The final bioconjugates PAMAM2-GSH and PAMAM4-GSH were obtained through freeze drying.

Physico-chemical characterization

FT-IR spectra were recorded on a Jasco 4200 spectrometer equipped with a Specac Golden Gate attenuated total reflectance (ATR) accessory, using a resolution of 4 cm^{-1} and an accumulation of 160 spectra, in the $4000\text{--}400\text{ cm}^{-1}$ wavenumber region. UV-VIS spectroscopy was performed on a CINTRA 101 double-beam spectrometer, at room temperature. The hydrodynamic diameters of the particles suspended in distilled water have been measured by dynamic light scattering (DLS) on a Zetasizer Nano ZS device from Malvern Instruments. Morphological information was obtained through scanning electron microscopy (SEM) of the gold-coated particles deposited onto aluminium-coated substrates. The analysis was performed using a QUANTA INSPECT F SEM device equipped with a field emission gun (FEG) with a resolution of $1,2\text{ nm}$ and with an X-ray energy dispersive spectrometer (EDS). The samples were also investigated using an Atomic Force Microscope (AFM) manufactured by Veeco, Multimode type. In order to not damage the surfaces and to reduce shear forces, the AFM system works in “tapping mode”. Roughness analysis was also performed in order to explore the functionalization with dendrimers. Calculation of the root mean square values (Ra) of surface profiles obtained, were performed using the NanoScope software, based on data obtained from previous image acquisition. Measurements were made on the entire area acquired ($10\text{ }\mu\text{m} \times 10\text{ }\mu\text{m}$).

Characterization of the PAMAM-modified particles

The first investigation of the success of the PAMAM-immobilization on the polymer particles was performed through ATR FT-IR, followed by the quantitative detection of the non-reacted dendrimer released during the dialysis of the PAMAM-treated materials. The applied procedure consists in the UV-VIS OPA method of detecting primary amines in solution. The reaction between $100\text{ }\mu\text{l}$ of analysis aliquot and OPA leads to a chromogene that specifically absorbs at 343 nm . Solutions of known concentrations of n-Bu in distilled water were used for the calibration curve. The amount of dendrimer was calculated through converting free amines into free PAMAM molecules. The efficiency - η of the PAMAM-modification was computed based on the amount of dendrimer released after the reaction, using the well-known equation:

$$\eta (\%) = (n_{\text{PAMAMi}} - n_{\text{PAMAMr}}) / n_{\text{PAMAMi}} * 100 \quad (1)$$

where n_{PAMAMi} and n_{PAMAMr} represent number of PAMAM moles introduced in the reaction system and released following the dialysis, respectively.

Thereafter, morphological and dimensional information was collected through DLS, SEM, and AFM.

Crosslinking assessment (Characterization of G2(4)-SPDP)

FT-IR was used to investigate the SPDP-activation of the materials.

UV-VIS spectrometry was used to quantitatively assess the success of the SPDP-activation. This method consisted in the monitoring of Py-2-thione formation during the treatment of the bioconjugation intermediate with reducing species like ME. Basically, if the coupling is successful, Py-2-thione forms via thiol disulfide exchange between the S-S-pyridyl group of PAMAM2(4)-SPDP and the -SH group from a thiol-containing species. Thus, excess of ME was added in a reactor containing a known amount of PAMAM2(4)-SPDP dispersed in PBS pH 7.4, under stirring. The reaction was allowed to occur for 24 hours, at room temperature. Then, the amount of Py-2-thione released was quantified through monitoring its characteristic absorption at 343 nm (fixed wavelength interrogation performed at room temperature). The molar concentration of Py-2-thione in the analyzed aliquot was calculated with the well-known equation:

$$C = \Delta A_{343\text{nm}} / (\epsilon_{\text{Py-2-thione}} \cdot \text{Path length}) \quad (2)$$

where $\Delta A_{343\text{ nm}}$ = average absorption A_{343} after the reaction with ME minus average A_{343} before adding ME; extinction coefficient for Py-2-thione $\epsilon = 8080\text{ M}^{-1}\text{cm}^{-1}$, path length = 1 cm. This allows to calculate the amount of Py-2-thione in the analyzed aliquot (which is equal with the S-S-py residues that have reacted with ME) and then to compare it with the total amount of SPDP used in the synthesis. Measurements were performed in triplicate.

Peptide coupling assessment

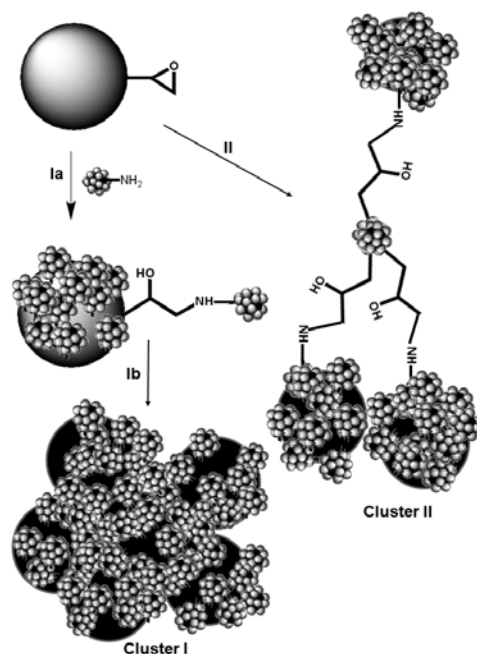
The generation of PAMAM2-GSH and PAMAM4-GSH bioconjugates was first investigated through FT-IR. The coupling of PAMAM2(4)-SPDP with the model thiol-terminated GSH was demonstrated by the UV-VIS quantitative detection of the total 2-Py-thione formed during that reaction. Basically, if the coupling is successful, 2-Py-thione is formed via thiol disulfide exchange between the -S-S-pyridyl group of PAMAM2(4)-SPDP and the -SH group of GSH. The amount of -S-S-pyridyl residues consumed is identical to the amount of -S-S-GSH linkages formed and to the released 2-Py-thione (1:1:1 molar). Hence, evaluating the amount of 2-Py-thione allows the immediate qualitative assessment of the success of the coupling and the quantitative determination of the degree of coupling. The success of the reaction was expressed as the percentage of PAMAM2(4)-GSH formed with respect to the total S-S-pyridyl from the in the PAMAM2(4)-SPDP used. UV-VIS experiments (under fixed wavelength mode at the specific wavelength for 2-Py-thione, 343 nm) were carried out to monitor the total side-reaction product. UV cells (1 cm pathlength) have been used.

25 mg PAMAM2(4)-SPDP was redispersed in 2 mL PBS pH 7.4 (using a ultrasonic bath Elma S30H) and then reacted with the appropriate volume of GSH solution in PBS pH 7.4 (concentration 2 mg/mL). The reaction media resulted at the end of the GSH-coupling have been filtered and measured at 343 nm, against the filtered dispersion medium of 25 mg bioconjugate dispersed in 2 mL PBS pH 7.4. The experiments were performed in triplicate. Solutions of 2-Py-thione of known concentrations were used to draw the calibration curve and to obtain the specific molar absorptivity. The coupling efficiency was estimated as the ration between the amount of bound GSH versus total -S-S-pyridyl groups in PAMAM2(4)-SPDP. The amount of bound GSH is given by the formed 2-Py-thione (in moles).

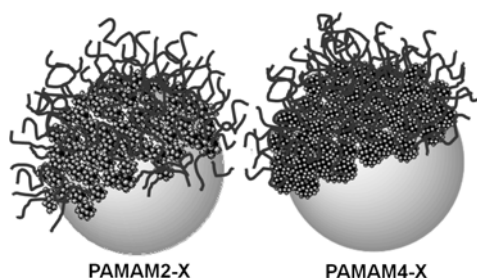
3. Results and discussion

The idea of using PAMAM as linker systems was due to the assumption that the highly functionalized outer sphere of the dendrimers macromolecules grafted on a solid support would improve the immobilization capacity of that support [11-14]. Nevertheless, the use of PAMAM should ensure both nanoroughness as well as multiamino- reactive sites.

In this context, it seemed of interest to investigate the influence of two generations of amino-ended dendrimers onto the surface properties of monodisperse polymer particles. Thus, it was expected that due to the dendrimers, the particles become not only nanostructured and functionalized, but modified beads should self-assemble forming clusters (as schematically suggested by Scheme 1). However, the remaining free amines are still available for enhanced cluster-like immobilization of different drugs, cell adherence peptides, growth hormones and/or other bioactive ingredients (Scheme 2).



Scheme 1. Schematic illustration of the reaction between amino- and epoxy- groups leading to the PAMAM surface-modification of P-GMA particles; route I: Ia – one PAMAM molecule reacts with a single epoxy- from just one P-GMA leading to nanorough amino-functionalized particles that may further agglomerate via hydrogen bonding leading to functionalized multimeric clusters (route Ib); route II – one PAMAM reacts with several particles behaving like a crosslinker and leading to nanorough clusters.



Scheme 2. Schematic illustration of PAMAM-grafted particles as cluster-type carrier for X biomolecules

The dendrimer-modified complex multimeric structures could present potential for further biofunctionalization followed by their physical loading into different biomaterials for a wide range of applications. There were two main practical problems addressed by the present work: 1) the first consisted in the engineering of nanorough particles of small dimensions and the influence of PAMAM on the morphology; 2) the second regards the insufficient availability of reaction sites and the solution provided here consists in a multifunctionalization intermediated by PAMAM linkers. It should be recalled that most of the procedures developed for the incorporation of active ingredients into scaffolds are based on non-covalent binding of the bioactive species. Physical techniques such as mixing, impregnation of hydrogels, layer-by-layer deposition as well as electrostatic interactions (based on charge compensation) were reported for the immobilization of a wide range of active ingredients in polymer-based matrices. These methods are suitable especially for controlled release applications, but also for tissue repair. However, for *in vivo* applications such as localized treatment and tissue reconstruction or regeneration, the chemical immobilization could provide important advantages, mainly due to longer and more stable contact of the physiological environment with the covalently bound bioactive ingredients, thus overcoming drug resistance or reduced effectiveness caused by continuous release.

From the point of view of the chemical immobilization, it is very important to control the interactions between the substrate and the active molecules. This is why this work aimed the development of a highly selective immobilization strategy of thiol-containing species onto SPDP-activated amines from the exterior shell of PAMAM-grafted particles.

PAMAM-modified particles; Influence of the generation on the roughness

The covalent binding of PAMAM was performed through a well known chemical affinity between amines and epoxy-groups [11, 15]. Basically, the beads were synthesized with an external epoxy-layer and thus the reaction with PAMAM occurred directly. The success of PAMAM immobilization was proved through FT-IR. The spectra of the control P-GMA samples presented typical absorptions for the chemical composition of the GMA-coated HEMA-St polymer. The broad stretching vibration of the hydroxyl from HEMA appeared at 3501 cm^{-1} . The peak specific for epoxy is not distinct visible probably because too many signals are overlapping in the wavenumber region around 1000 cm^{-1} . This is normal to occur because the GMA-layer is very thin and the particles themselves have very small dimensions. Figure 1 displays the most important spectral modifications. One may expect to see the consumption of epoxy groups from P-GMA simultaneously with the appearance of new hydroxyl leading to a spectral intensification at above $3500\text{-}3400\text{ cm}^{-1}$, together with amine and amide vibrations from the dendrimers. The first expected change is impossible to be observed since the epoxy-vibration was not distinct in the control spectrum. The spectra of P-PAMAM2 and P-PAMAM4 have indicated two new absorptions at 1649 and 1552 cm^{-1} assigned as amide I and amide II vibrations due to the dendrimer presence onto the surface. These are the main diagnostic peaks proving the dendrimer presence onto the polymer surface. Nevertheless, strong and broad vibrations assigned to the overlapping hydroxyl and N-H are visible on the spectra of the PAMAM-treated polymers at 3501 and 3303 cm^{-1} respectively. The first signal is due to O-H of mixed origin (from HEMA units and newly formed in the reaction amine-epoxy) and the second one to N-H stretching from -NH_2 and amides. The O-H vibration from HEMA units is still detectable after the coating with GMA and even following the dendrimer-grafting because of the undermicronic overall dimension of the polymer bead; this makes that the infrared spectrum is collected from the whole material, not only at its very thin surface.

These results confirm the dendrimers presence on the polymer particles. This is in agreement with the result of the indirect UV-VIS quantitative assessment of the PAMAM binding. No non-reacted amines have been detected in the dialysis media, suggesting a 100% reaction efficiency of the PAMAM binding.

With respect to the morphology investigation, P-GMA have been obtained as stable latex with polymer beads presenting very low polydispersity (as proved by DLS measurements indicating an average diameter (a.d.) of $315.1 \pm 2.179\text{ nm}$ and a polydispersity index of 0.032 ± 0.027). Following the dendrimer treatment, the stability of the latex was lost and a precipitation occurred suggesting thus a drastic increase of particles' dimension and mass. This behavior was confirmed through DLS, the a.d. of the structures obtained following the PAMAM-treatment increasing to more than 2000 nm for P-PAMAM2 and to more than 2500 nm for P-PAMAM4 (as displayed in Figure 2).

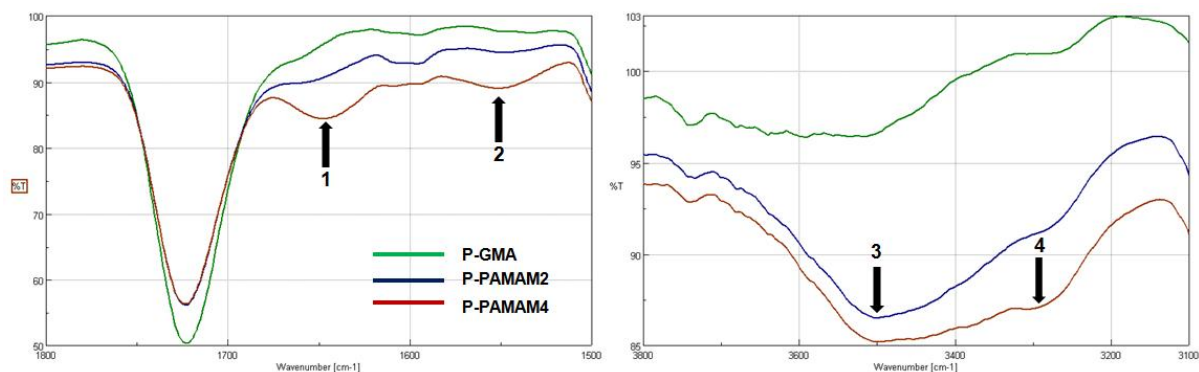


Fig. 1. FT-IR detail of the spectral modifications following the dendrimer-treatment. 1 – amide I ($C=O$ stretching vibration); 2 – amide II ($C-N$ stretching and $N-H$ bending); 3 – $O-H$ stretching and 4 – amine and amide $N-H$ stretching.

This important dimensional modification could not be due to a simple surface binding of dendrimers onto the surface of a polymer bead. Dendrimers are indeed globular molecules but the calculated diameters of the species used here are described by Dendritech to be lower than 5 nm. Since PAMAM interacts exclusively at the exterior of the particles, two mechanisms are presumed to occur, as depicted in Scheme 1. The first one consists in the assembling of PAMAM-modified single particles, through physical interactions, into complex multimeric structures with amino-reactive outer-shell (see cluster I in Scheme 1). The second one presumes that PAMAM molecules behave like crosslinkers between several particles, leading to chemically linked clusters (see cluster II in Scheme 1). We do not exclude the second possibility, but the DLS results indicating quite homogeneous structures with low polydispersity (polydispersity index of 0.176 ± 0.104 for P-PAMAM2 and 0.153 ± 0.120 for P-PAMAM4) state more for the first proposed mechanism. More morphological details have been available through SEM. P-GMA particles were monodisperse in size and shape. Their dimensions were lower than the corresponding a.d. obtained through DLS since SEM was performed on dried particles. Very interesting, for P-PAMAM2 and P-PAMAM4, respectively, individual PAMAM-grafted beads were evidenced through SEM, and the existence of cluster-like agglomerations of particles was suggested (see panels b and panels c in Figure 2). The dimension of these aggregates seems to match the dimensions obtained by DLS. No cluster or other agglomeration of particles was visible for the control P-GMA sample. Nano-features with dimensions ranging from 50 to 70 nm are visible onto the PAMAM-grafted beads. These probably consist in agglomerated dendrimer macromolecules reacted onto the polymer epoxy shell. Moreover, the dendrimer-modified beads present higher roughness with increasing the dendrimer generation, when compared to the control P-GMA substrate.

The investigation of the roughness modification following the PAMAM-treatment has been performed through AFM. The analysis confirmed the existence of individual particles and it has indicated an increased roughness from 19.8 nm for the substrate to 25.7 nm for P-PAMAM2 and 46 nm for P-PAMAM4. Figure 3 is suggestive with this respect displaying the topography of dried polymer particles before and after the modification with dendrimers. Both dimensions and roughness augmented following the dendrimer treatment, stating for the successful modification of the polymer particles with PAMAM. This is in agreement with the SEM data.

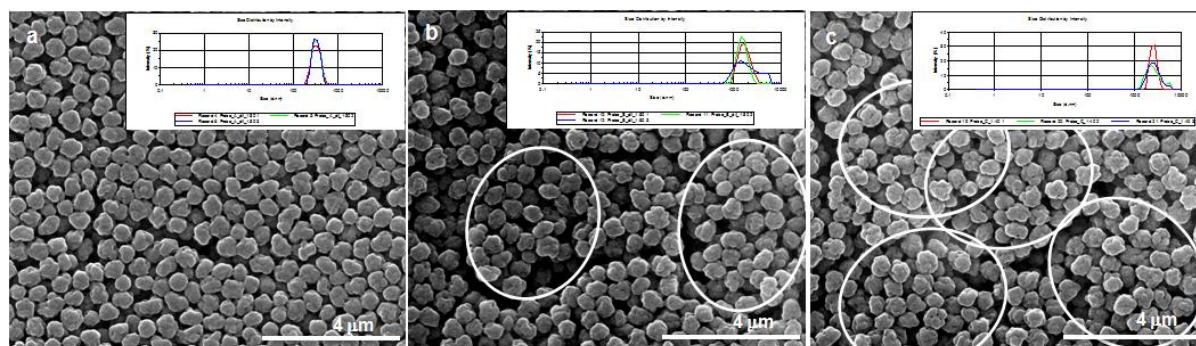


Figure 2. Morphology of the PAMAM-modified particles versus control P-GMA. SEM images and DLS measurements of a) P-GMA - monodisperse particles, $a.d. = 315.1 \pm 2.179$ nm; b) P-PAMAM2 - modified particles organized as clusters with $a.d. = 2114 \pm 65.48$ nm; c) P-PAMAM4 - modified particles organized as clusters with $a.d. = 2663 \pm 223.5$ nm.

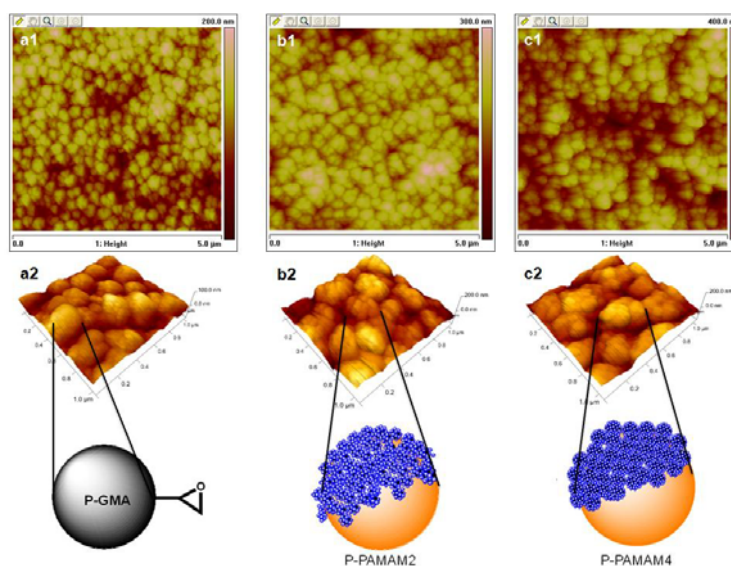


Figure 3. Surface morphology obtained through AFM. 2D view of a1) P-GMA; b1) P-PAMAM2; c1) P-PAMAM4 and 3D detail at $1 \mu\text{m} \times 1 \mu\text{m}$: a2) P-GMA; b2) P-PAMAM2; c2) P-PAMAM4. A schematic detail of the modified particles is provided for each material.

Evaluation of the $-\text{NH}_2$ activation with SPDP

The investigation of the SPDP-treated samples through FT-IR has successfully proved the modification of the dendrimer-grafted particles. The diagnose peak considered suggestive with this respect is the new absorption at approximately 450 cm^{-1} assigned to the S-S vibration from the dithio-pyridine residue of the SPDP-treated particles. Figure 4 presents this spectral modification.

Furthermore, UV-VIS successfully proved the formation of Py-2-thione following the treatment of the SPDP-treated particles with ME. This information is very important for the success of the SPDP-crosslinking since it gives a quantitative aspect to the crosslinking efficiency. It was proved that 86% of the SPDP used to modify P-PAMAM2 has been linked; in the same way it was demonstrated that 60% of the SPDP used to activate P-PAMAM4 has reacted. These results are encouraging for the potential of these materials as biofunctional carriers, since we have used for the activation only low ratio between SPDP and free amines from the dendrimer-grafted material. However, further work should be devoted to the deeper exploring and advanced control of the activation reaction.

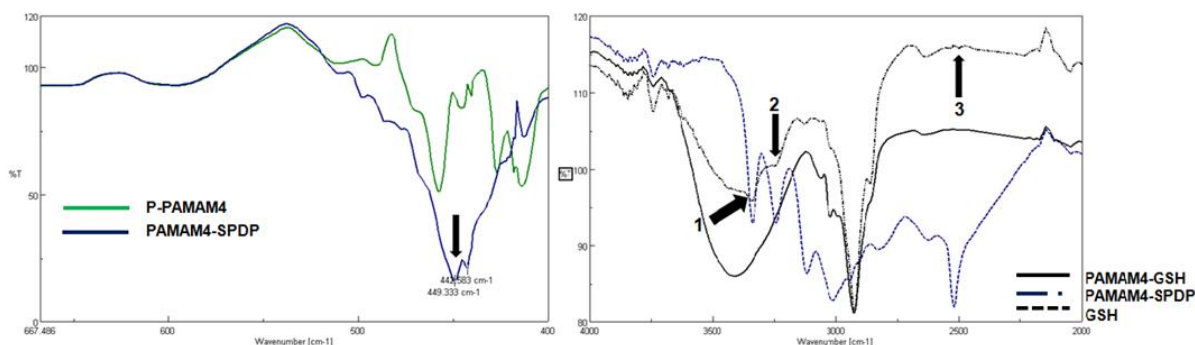


Figure 4. FT-IR detail revealing: left - SPDP-modification of P-PAMAM4; right - main spectral modifications recorded following the peptide coupling against control GSH and PAMAM4-SPDP. 1 –O-H vibration from the carboxyl groups in GSH; 2 – N-H vibration due to the amines from GSH; 3 – disappearance of the S-H vibration characteristic for GSH in the final bioconjugate. The last modification represents the main evidence of the chemical coupling.

Peptide coupling

GSH successful coupling was first qualitatively evidenced through FT-IR as depicted in Figure 4. The main evidence consists in new peaks due to the immobilized peptide from the PAMAM-GSH bioconjugate and the lack of the S-H vibration characteristic to free GSH. Thus, the shifting of the peak displayed at 3412 in PAMAM-SPDP intermediates to 3440 cm^{-1} in PAMAM-GSH bioconjugates is observed. This is due to the O-H vibrations from the carboxylic groups of the peptide. Moreover, two new peaks, distinguishing from the broad signal resulted from the overlapping of O-H and N-H vibrations in PAMAM-SPDP are visible at 3343 and 3240 cm^{-1} , respectively (arrows 1 and 2 in Figure 4). These modifications are due to the N-H stretching due to NH_2 and amide groups from the peptide. Very important, the S-H stretching vibration at 2501 cm^{-1} , has disappeared from the resulting coupled PAMAM-GSH bioconjugate; this is a very strong evidence of the peptide coupling. Nevertheless, S-S vibration at about 450 cm^{-1} (characteristic for SPDP-containing intermediates) is still visible in the spectrum of the bioconjugate. Amide I and II are also increasing in intensity due to the corresponding groups from the peptide when compared to the SPDP-containing intermediate (data not shown).

Furthermore, the coupling efficiency has been proved through UV-VIS detection of the Py-2-thione formed during the coupling reaction. The results have proved that GSH was 100% chemically linked to the bioconjugation PAMAM-SPDP intermediates. This means that all the pyridil-dithio residues from the intermediates reacted with GSH. These results confirm the high reactivity of the active intermediates against thiol-bearing species.

4. Conclusions

Multifunctional amino-particles with nanorough surfaces were created through PAMAM immobilization on polymer beads. The stability of the original latex was lost following PAMAM-treatment, since the dendrimer-grafted beads self-assemble into complex multimeric structures with amino-reactive outer-shell. Their nanoroughness and the reactivity increased with the generation of the dendrimers. In the second part of this work, the resulted materials were used to demonstrate their further potential for highly selective reactivity with respect to thiol-ended species. Thus, in a first step, a thiol-selective heterobifunctional reagent (namely SPDP) was used to activate the free amines from P-PAMAM substrates. Then, the obtained intermediates were coupled with a model peptide, GSH. The bioconjugation efficiency and the high reactivity of the PAMAM-containing particles were successfully demonstrated. Further studies will be devoted to a deeper control of the coupling chemistry. The dendrimer-modified complex multimeric structures

are promising candidates for biofunctionalization followed by physical loading into different biomaterials for a wide range of HT applications.

Acknowledgements

This work was supported by CNCSIS – UEFISCSU, project number PNII – IDEI code 248/2010.

References

- [1] S. Kay, A. Thapa, K.M. Haberstroh, T.J. Webster, *Tissue Eng.* **8**, 753 (2002).
- [2] J.Y. Martin, Z. Schwartz, T.W. Hummert, D.M. Schraub, J. Simpson, J. Lankford Jr., D.D. Dean, D.L. Cochran, B.D. Boyan, *J. Biomed. Mater. Res.* **29**, 389 (1995).
- [3] U. Meyer, A. Buechter, A. Wiesmann, U. Joos, D.B. Jones, *Eur. Cell. Mater.* **9**, 39 (2005).
- [4] V. Perla, T.J. Webster, *J. Biomed. Mater. Res. Part A*, **75A**(2), 356 (2005).
- [5] R.L. Price, C. Ellison, K.M. Haberstroh, T.J. Webster, *J. Biomed. Mater. Res.* **70**, 129 (2004).
- [6] R.L. Price, K.M. Haberstroh, T.J. Webster, *Med. Biol. Eng. Comput.* **41**, 372 (2003).
- [7] R.L. Price, M.C. Waid, K.M. Haberstroh, T.J. Webster, *Biomaterials* **24**, 1877 (2003).
- [8] B.C. Ward, T.J. Webster, *Biomaterials* **27**, 3064 (2006).
- [9] B.C. Ward, T.J. Webster, *Mater. Sci. Eng.: C* **27**, 575 (2007).
- [10] S. Wu, X. Liu, T. Hu, P.C. Chu, J.P.Y. Ho, Y.L. Chan, K.W.K. Yeung, C.L. Chu, T.F. Hung, K.F. Huo, C.Y. Chung, W.W. Lu, K.M.C. Cheung, K.D.K. Luk, *Nano Letters* **8**(11), 3803 (2008).
- [11] R. Benters, C.M. Niemeyer, D. Drutschmann, D. Blohm, D. Woehrle, *Nucl. Acids Res.* **30**(2) E10.
- [12] F.N. Crespilho, M.E. Ghica, M. Florescu, F.C. Nart, O.N. Oliveira Jr, C.M.A. Brett, *Electrochem. Commun.* **8**, 1665 (2006).
- [13] I.C. Stancu, *React. Funct. Polym.* **70**(5), 314 (2010).
- [14] S. Wang, P. Su, E. Hongjun, Y. Yang, *Anal. Biochem.* (2010) DOI 10.1016/j.ab2010.06.014.
- [15] G.T. Hermanson, *Bioconjugate Techniques*, 2nd Edition, Academic Press, Inc. (2008)
- [16] E. Rusen, A. Mocanu, B. Marculescu, C. Andronescu, I.C. Stancu, A. Ionca, I. Antoniac, Influence of the solid-liquid adhesion on the self-assembling properties of colloidal particles, in: V.E. Laine (Ed.), *Photonic Crystals: Fabrication, Band Structure and Applications*, NOVA PUBLISHERS 2010.